

Doubly resonant second harmonic generation of 2.0 μm light in coupled InGaAs/AlAs quantum wells

H. C. Chui, E. L. Martinet, G. L. Woods, M. M. Fejer, and J. S. Harris, Jr.
Center for Nonlinear Optical Materials Research, McCullough 226, Stanford University, Stanford,
California 94305-4055

C. A. Rella, B. I. Richman, and H. A. Schwettman
Stanford Picosecond FEL Center, W. W. Hansen Experimental Physics Laboratory, Stanford University,
Stanford, California 94305-4085

(Received 2 February 1994; accepted for publication 20 April 1994)

We demonstrate intersubband absorption and second harmonic generation (SHG) in asymmetric coupled $\text{In}_{0.6}\text{Ga}_{0.4}\text{As}/\text{AlAs}$ n -type quantum wells (QWs) grown on a GaAs substrate. Intersubband absorption at 4.1 and 2.1 μm wavelengths, corresponding to the 1 to 2 and 1 to 3 transitions, respectively, are observed. SHG of 2.0 μm light is demonstrated in this doubly resonant QW. This is the shortest wavelength SHG to date in any n -type QW system. The second order nonlinear susceptibility $\chi^{(2)}$ is measured using a free electron laser by interference of the second harmonic fields from the QW and substrate. At a pump wavelength of 4.0 μm , a large asymmetry in the SHG power with rotation angle of the sample arising from SHG from the QW is observed, and a $\chi^{(2)}$ of magnitude $20 \pm 8 \text{ nm/V}$, approximately 100 times that of bulk GaAs, and phase $63^\circ \pm 34^\circ$ relative to the GaAs substrate is measured. Comparison of both the linear and nonlinear properties to a simple model is discussed.

Quantum wells (QWs) have been demonstrated to have extremely large nonlinear susceptibilities arising from intersubband transitions.¹⁻⁴ These large nonlinear susceptibilities may result in efficient nonlinear optical frequency conversion and electro-optic switching devices.⁵ These intersubband transitions are typically limited to the far and mid-infrared, but recent advances in strained QW materials have allowed intersubband transition energies in n -type QWs to reach the technologically important 2 μm wavelength,^{6,7} where compact InGaAsP and GaSb diode laser sources⁸ as well as diode pumped Tm:Ho:YAG lasers are available. However, the nonlinear optical properties from these short wavelength intersubband transitions have only begun to be investigated.⁹ In this work, we report both intersubband absorption and second harmonic generation (SHG) of 2 μm light in asymmetric coupled InGaAs/AlAs QWs.

The asymmetric coupled QW structure used for these studies was designed to be doubly resonant for efficient SHG. The QW subband eigenstates were modeled with a single band effective mass model with nonparabolicity included using an energy-dependent effective mass as described previously.⁷ Band bending was not taken into account. The coupled QW consisted of two heavily doped (sheet charge density of $3.0 \times 10^{12} \text{ cm}^{-2}$ per coupled QW) $\text{In}_{0.6}\text{Ga}_{0.7}\text{As}$ wells of 31.1 and 12.7 \AA thicknesses separated by a 5.65 \AA AlAs intermediate barrier. One monolayer of GaAs was added to either end of the double well to smooth the interfaces between the AlAs barrier and InGaAs wells.¹⁰ The band diagram of the coupled quantum well with calculated subband energies and wave functions is shown in Fig. 1. The calculated intersubband transition energies and dipole moments are $E_{12}=297 \text{ meV}$, $E_{13}=523 \text{ meV}$, $z_{12}=9.7 \text{ \AA}$, $z_{13}=-6.0 \text{ \AA}$, $z_{22}-z_{11}=21.1 \text{ \AA}$, and $z_{23}=11.0 \text{ \AA}$. 200 periods of the coupled QWs separated by 100 \AA AlAs barriers were grown on a (100) semi-insulating GaAs substrate by molecular beam epitaxy (MBE) in a Varian Gen II system. A

linearly graded InGaAs buffer with a final indium composition of 30% was used to provide strain compensation in the QWs.^{11,12} The sample was grown at a substrate temperature of 375 $^\circ\text{C}$ with As_4 . Details of the growth studies used to optimize the growth conditions for $\text{In}_{0.5}\text{Ga}_{0.5}\text{As}/\text{AlGaAs}$ QWs are given elsewhere.¹⁰

The intersubband absorption of the sample was measured using a Fourier transform infrared (FTIR) spectrometer with the sample mounted at Brewster's angle to the TM polarized light. The absorption spectrum of the sample is shown in Fig. 2. Absorption peaks at $E_{12}=300 \text{ meV}$ (4.1 μm) and $E_{13}=580 \text{ meV}$ (2.1 μm) are observed. To our knowledge, this is the largest E_{13} reported to date. These measured intersubband energies are within 10% of the theoretically predicted values. Lorentzian lineshapes fit to the absorption peaks yield half-width at half-maximum (HWHM) linewidths of $\Gamma_{12}=41 \text{ meV}$ and $\Gamma_{13}=67 \text{ meV}$ and integrated absorption fractions (IAFs) of 28.1 and 9.8 mAbs meV/QW for the 1 to 2 and 1 to 3 transitions, respectively. Assuming $z_{12}=9.7 \text{ \AA}$ from theory, the measured IAFs

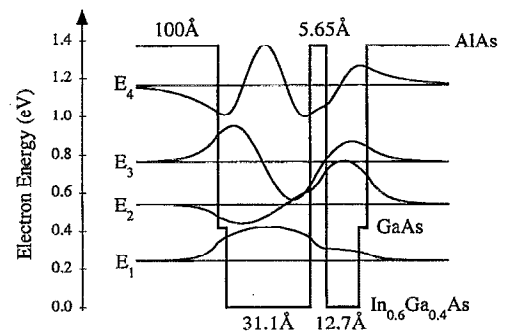


FIG. 1. Conduction band diagram of the asymmetric coupled QW with calculated subband energies and wave functions.

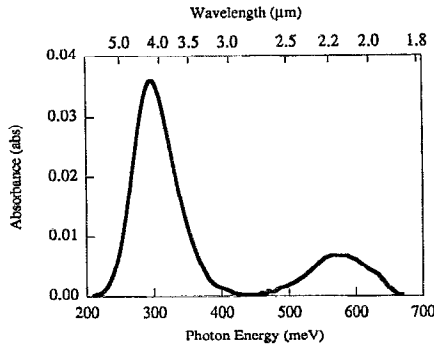


FIG. 2. Absorption spectrum of the coupled QW showing intersubband absorption peaks at 4.1 and 2.1 μm wavelengths corresponding to the 1 to 2 and 1 to 3 transitions, respectively.

yield an effective doping concentration $\sigma_{\text{eff}} = 3.0 \times 10^{12} \text{ cm}^{-2}/\text{QW}$ and $|z_{13}| = 4.2 \text{ \AA}$.¹³

The second order nonlinear susceptibility $\chi^{(2)}$ of the QW, $\chi_{\text{QW}}^{(2)}$, can be calculated by treating the QW as a three-level system. If the i th subband to j th subband transition has a Lorentzian line shape with dipole moment z_{ij} and HWHM linewidths of Γ_{ij} , then near double resonance, $\chi^{(2)}$ is given by¹⁴

$$\chi_{\text{QW}}^{(2)} \approx \frac{2q^3 N_{\text{eff}}}{\epsilon_0} \sum_{m,n} \frac{z_{1n} z_{nm} z_{m1}}{(\hbar\omega - E_{1n} - i\Gamma_{1n})(2\hbar\omega - E_{1m} - i\Gamma_{1m})}, \quad (1)$$

where only the ground state subband is assumed to be occupied with a carrier concentration, N_{eff} . This formulation neglects inhomogeneous broadening of the intersubband transitions as well as local field effects due to charge screening in the QW layers. Using the intersubband transition parameters derived from the intersubband absorption measurement, $N_{\text{eff}} = \sigma_{\text{eff}}/l_{\text{QW}}$, where $l_{\text{QW}} = 155.1 \text{ \AA}$ is the QW period, and assuming $z_{22} - z_{11} = 21.1 \text{ \AA}$ and $z_{23} = 11.0 \text{ \AA}$ from theory, an estimate for $\chi_{\text{QW}}^{(2)}$ is obtained. The calculated magnitude and phase of $\chi_{\text{QW}}^{(2)}$ is shown in Fig. 3. The double resonant peak of the $\chi_{\text{QW}}^{(2)}$ is near 4.5 μm wavelength with a magnitude of 12 nm/V .

SHG measurements were performed with a free electron laser (FEL) tuned to a wavelength of 4.0 μm . The Stanford FEL¹⁵ generates pulses with pulse lengths of a few picoseconds, a peak power of several hundred kilowatts, and a linewidth of approximately 10 nm. The pump beam was focused onto the sample with a focal spot diameter of 100 μm . The QW and reference samples were placed in a rotation stage which allowed varying the incidence angle θ and rotating in angle ϕ about the sample normal. Multilayer dielectric filters were placed both before and after the sample in order to prevent incident 2.0 μm radiation from the FEL from reaching the sample and to block the 4.0 μm pump radiation from reaching the detector, respectively. The power leakage through the filters at the blocking wavelengths was determined to be below the detector noise level. ZnSe polarizers were used on both the input and collection side to select only the TM polarization. A PbS detector was used to measure the SHG signal. In addition, a portion of the FEL pump beam

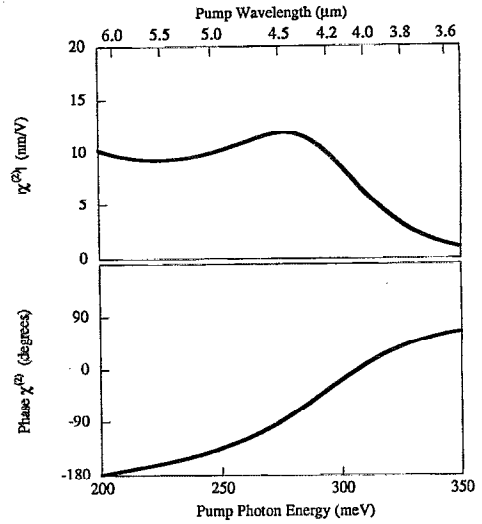


FIG. 3. Calculated spectrum of the magnitude (top graph) and phase (bottom graph) of SHG $\chi^{(2)}$ for the coupled QW.

was focused onto a properly phase matched AgGaSe₂ crystal and detected with an InSb detector for use as a reference SHG signal. The measured SHG power was then normalized to fluctuations in the pump power by dividing by the reference SHG signal.

$\chi_{\text{QW}}^{(2)}$ was measured by mixing the second harmonic (SH) from the QW with the SH from the GaAs substrate.¹⁴ Since the symmetry of $\chi^{(2)}$ in bulk GaAs is different than that in QWs, polarization selection can be used to extract $\chi_{\text{QW}}^{(2)}$. The $\chi_{\text{QW}}^{(2)}$ tensor has a nonzero (zzz) element, and the $\chi_{\text{GaAs}}^{(2)}$ tensor has a nonzero (xyz) element. If only the TM polarization is selected, the SHG conversion at frequency ω from the QW sample is given by⁹

$$\frac{I_{2\omega}}{I_{\omega}^2} \propto \left| \chi_{\text{GaAs}}^{(2)} \cos 2\phi \sin \zeta e^{i\zeta} + \frac{\pi l_{\text{MQW}} \sin^2 \theta_{\text{int}}}{6l_c \cos^2 \theta_{\text{int}}} \chi_{\text{QW}}^{(2)} \right|^2, \quad (2)$$

where $I_{2\omega}$ and I_{ω} are the SH and pump intensities, ϕ is the angle between the projection of the pump beam onto the sample and the (110) direction of the sample, θ is the incidence angle (angle between the sample normal and the pump beam) with internal angle θ_{int} , l_{MQW} is the total thickness of the MQW layers,

$$\zeta \approx \frac{\pi}{2} \frac{L}{l_c \cos \theta_{\text{int}}} \quad (3)$$

is half the phase mismatch between the pump and SH fields, L is the total thickness of the combined MQW and substrate, and

$$l_c = \frac{\pi c}{2\omega(n_{2\omega} - n_{\omega})} \quad (4)$$

is the coherence length in GaAs. For our sample, $l_{\text{MQW}} = 3.1 \mu\text{m}$ and $L = 401 \mu\text{m}$. Then, if l_c is known with sufficient accuracy, $\chi_{\text{QW}}^{(2)}$ can be extracted by measuring the SHG conversion efficiency versus angle ϕ and fitting to Eq. (2).

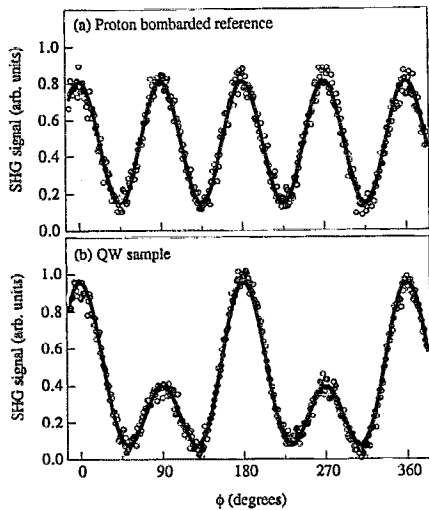


FIG. 4. Measured (hollow circles) and theoretically fitted (solid lines) normalized SHG power vs rotation angle ϕ for the proton bombarded reference (top graph) and QW sample (bottom graph) at a pump wavelength of $4.0 \mu\text{m}$.

The value of l_c can be obtained via Eq. (4) by using published values of the refractive index of GaAs.¹⁶ However, an accuracy of 10^{-3} for the indices of refraction yields an accuracy of only $\pm 10\%$ on l_c . By using a wedge technique,^{14,17} we determined that the coherence length l_c is $44.7 \pm 2.1 \mu\text{m}$ and $52.7 \pm 1.8 \mu\text{m}$ at 4.8 and $5.19 \mu\text{m}$ wavelengths, respectively. The values of l_c calculated from the refractive index data lie within the error bars of these directly measured values. Thus, we have confidence in assuming that $l_c = 28.86 \mu\text{m}$ to an accuracy of $\pm 4\%$ at $4.0 \mu\text{m}$ as calculated from the refractive index data.

We measured the normalized SHG power versus angle ϕ for both the QW sample and a proton bombarded QW sample for reference (proton bombardment causes trapping of the conduction band electrons so that $\chi_{\text{QW}}^{(2)}$ is zero³). These ϕ scans were taken at $\theta = 45^\circ$ and are shown in Fig. 4. The proton bombardment reference has even peaks of 0° , 90° , 180° , and 270° arising, respectively, from alignment of the incident polarization to the (110) , $(\bar{1}10)$, $(1\bar{1}0)$, and $(\bar{1}\bar{1}0)$ crystal directions of the GaAs. As also shown in Fig. 4(a), this reference ϕ scan fits a $\cos^2(2\phi)$ dependence. The QW sample, on the other hand, has a large asymmetry in the ϕ scan with stronger 0° and 180° peaks than 90° and 270° peaks. This large asymmetry is due to addition of the ϕ -independent QW SH field to the ϕ -dependent substrate SH field, so that the resulting intensity follows a $(\cos 2\phi + \text{constant})^2$ dependence as given in Eq. (2). By fitting the QW ϕ scan to Eq. (2) with a complex $\chi_{\text{QW}}^{(2)}$ fitting parameter, while allowing for variations of $\pm 4\%$ in l_c and $\pm 5\%$ of the maximum signal as an offset of the signal due to uncertainty in the baseline of the SHG signal, $\chi_{\text{QW}}^{(2)}$ of magnitude $20 \pm 8 \text{ nm/V}$ and phase $63^\circ \pm 34^\circ$ was determined. This measured $|\chi_{\text{QW}}^{(2)}|$ is approximately 100 times the value of $\chi_{\text{GaAs}}^{(2)}$ (Ref. 18) and is larger than the theoretical peak of 12 nm/V . Further reductions in the uncertainty in l_c and SHG signal baseline would significantly improve the accuracy in the phase and magnitude. Since the line shapes are not perfect Lorentzians, differences between theory and measure-

ment may arise. Inaccuracies in the measured 1–3 intersubband energy and linewidth, local field effects, and inaccuracies in the theoretical z_{23} may also contribute to the inaccuracy in the theoretical estimate for $\chi_{\text{QW}}^{(2)}$.

In conclusion, we have demonstrated intersubband absorption in asymmetric coupled $\text{In}_{0.6}\text{Ga}_{0.4}\text{As}/\text{AlAs}$ QWs at 4.1 and $2.1 \mu\text{m}$ wavelengths, among the shortest wavelength intersubband absorption to date. The measured absorption peak energies are within 10% of the theoretical values. We have also demonstrated SHG of $2.0 \mu\text{m}$ light using these QWs. This is the shortest wavelength SHG to date in any n -type QW system. Using a FEL tuned to $4.0 \mu\text{m}$ wavelength as the pump source, a $\chi^{(2)}$ of magnitude $20 \pm 8 \text{ nm/V}$, approximately 100 times that of bulk GaAs, is measured. Future SHG measurements at different wavelengths should help to determine the dispersion of $\chi_{\text{QW}}^{(2)}$ so that a more rigorous comparison to theory can be made. With these short wavelength intersubband transitions, InGaAs/AlGaAs QWs should be useful for nonlinear optical frequency conversion using diode laser sources near $2 \mu\text{m}$.

H. C. Chui acknowledges fellowship support from the Office of Naval Research (ONR) and Center for Nonlinear Optical Materials (CNOM), E. L. Martinet, from ONR and Lockheed, and G. L. Woods, from CNOM. This work was supported by ONR under Contract No. N00014-91-C-0170 and Contract No. N00014-92-J-1903, by ARPA under Contract No. N00014-90-J-4056, and CNOM under Contract No. N00014-92-J-1903. FTIR measurements were performed on a Bruker FTIR at the Stanford Free Electron Laser facility.

- ¹M. M. Fejer, S. J. B. Yoo, R. L. Byer, A. Harwit, and J. S. Harris, Jr., *Phys. Rev. Lett.* **62**, 1041 (1989).
- ²E. Rosencher, P. Bois, J. Nagle, and S. Delaitre, *Electron. Lett.* **25**, 1041 (1989).
- ³S. J. B. Yoo, M. M. Fejer, R. L. Byer, and J. S. Harris, Jr., *Appl. Phys. Lett.* **58**, 1724 (1991).
- ⁴C. Sirtori, F. Capasso, D. L. Sivco, S. N. G. Chu, and A. Y. Cho, *Appl. Phys. Lett.* **59**, 2302 (1991).
- ⁵J. Khurgin, *J. Opt. Soc. Am. B* **6**, 1673 (1989).
- ⁶Y. Hirayama, J. H. Smet, L. H. Peng, C. G. Fonstad, and E. P. Ippen, *Appl. Phys. Lett.* **63**, 1663 (1993).
- ⁷H. C. Chui, E. L. Martinet, M. M. Fejer, and J. S. Harris, Jr., *Appl. Phys. Lett.* **64**, 736 (1994).
- ⁸H. K. Choi, S. J. Eglash, and M. K. Connors, *Appl. Phys. Lett.* **63**, 3271 (1993).
- ⁹E. L. Martinet, G. L. Woods, H. C. Chui, J. S. Harris, Jr., M. M. Fejer, C. A. Rella, and B. A. Richman, in *SPIE Proceedings: Quantum Well and Superlattice Physics V* (1994), Vol. 2139.
- ¹⁰H. C. Chui and J. S. Harris, Jr., *J. Vac. Sci. Technol. B* **12**, 1019 (1994).
- ¹¹S. M. Lord, B. Pezeshki, and J. S. Harris, Jr., *Electron. Lett.* **28**, 1193 (1992).
- ¹²H. C. Chui, S. M. Lord, E. Martinet, M. M. Fejer, and J. S. Harris, Jr., *Appl. Phys. Lett.* **63**, 364 (1993).
- ¹³L. C. West and S. J. Eglash, *Appl. Phys. Lett.* **46**, 1156 (1985).
- ¹⁴Y. R. Shen, *The Principles of Nonlinear Optics* (Wiley, New York, 1984).
- ¹⁵T. I. Smith, H. A. Schwettman, K. W. Berryman, and R. L. Swent, in *SPIE Proceedings: Free Electrons Laser Spectroscopy in Biology, Medicine, and Material Science*, edited by H. A. Schwettman, 1993, Vol. 1854, pp. 23–33.
- ¹⁶A. N. Pikhtin and A. D. Yas'kov, *Sov. Phys. Semicond.* **12**, 622 (1978).
- ¹⁷S. K. Kurtz, in *Quantum Electronics Volume I: Nonlinear Optics, Part A*, edited by H. Rabin and C. L. Tang (Academic, New York, 1975), pp. 209–281.
- ¹⁸B. F. Levine and C. G. Bethea, *Appl. Phys. Lett.* **20**, 272 (1972).